
Complexes of Dichloro(Ethylenediamine)Palladium(II) Observed from Aqueous Solutions by Electrospray Mass Spectrometry

Stephan B. H. Bach, Cassandra E. Green, Linda I. Nagore,
Tiffanee G. Sepeda, and Grant N. Merrill

Department of Chemistry, The University of Texas at San Antonio, San Antonio, Texas, USA

Aqueous solutions of dichloro(ethylenediamine)palladium(II) were investigated using electrospray mass spectrometry (ESMS). The most abundant peak (m/z 436.8) was attributed to the dimeric $\text{Pd}(\text{en})\text{Cl}_2\text{-Pd}(\text{en})\text{Cl}^+$ ion. We conjecture that the structures of the observed ions arise from the clustering of the hydrolysis products of the parent compound. This hypothesis was tested experimentally by carrying out a series of collision-induced dissociation (CID) experiments and deuterium exchange reactions. It was also assessed by performing density functional theory (DFT) calculations, from which optimized structures and reaction energetics were obtained. These results were compared with our earlier ESMS study of an aqueous $\text{Pd}(\text{en})\text{Br}_2$ solution. Calculations were also carried out on the $\text{Pd}(\text{en})\text{Br}_2$ system to facilitate the comparisons. Conclusions are drawn regarding the species present in the two aqueous solutions. (J Am Soc Mass Spectrom 2007, 18, 769–777) © 2007 American Society for Mass Spectrometry

The last decade has seen a resurgence of interest in the coordination chemistry of transition metals. This is due in large part to their therapeutic value as antitumor agents. Many of these agents are platinum(II) complexes, the four best known being cisplatin, carboplatin, oxaliplatin, and nedaplatin [1–3]. Palladium(II) complexes have also attracted attention for similar reasons [4–7].

In vivo, hydrolysis of these compounds occurs, and it is these hydrolytic products that yield their medicinal activity [8, 9]. The hydrolytic products are also strongly linked to issues of renal toxicity [10]. The mechanisms of action for these coordination complexes are closely tied to their hydrolysis products, and these products and mechanisms are poorly understood, partly due to the possibility of multiple equilibria with similar energetics [11, 12]. It is for these reasons that coordination complexes of Ni(II), Pd(II), and Pt(II) in aqueous solutions have been the focus of a number of investigations [13–17].

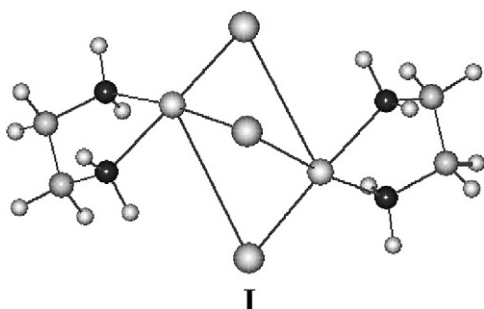
Electrospray mass spectrometry (ESMS) is particularly well suited for the study of metal-containing aqueous solutions, and a variety of such studies have been conducted [18, 19]. We recently reported the results of one such study into aqueous solutions of

dibromo(ethylenediamine)palladium(II) [20]. When the solution was electrosprayed into a quadrupole ion-trap mass spectrometer, a number of previously unreported species were detected, the principle one being a dimeric ion formed from the $\text{Pd}(\text{en})\text{Br}_2$ parent compound and the $\text{Pd}(\text{en})\text{Br}^+$ ion. The dimeric ion was subjected to collision-induced dissociation (CID), and these MS^n experiments revealed a series of ions formed through the sequential loss of HBr molecules. Complexes observed from the electrospray process are not necessarily a reflection of those complexes in solution, but they may instead simply represent species in solution from which the complexes are produced in the electrospray desolvation process. This has been observed previously in solutions containing mixtures of charged and neutral species [21]. Coupled with these experimental results, density functional theory (DFT) calculations were carried out to determine the structure of the principal ion, which was found to be a bromo-bridged compound of $\text{Pd}(\text{en})\text{Br}_2$ and $\text{Pd}(\text{en})\text{Br}^+$ (I).

We have continued this series of investigations and report the results of an ESMS study of aqueous solutions of $\text{Pd}(\text{en})\text{Cl}_2$ involving both CID and deuterium exchange experiments. Extensive DFT calculations have also been carried on all the observed ions and related species in an attempt to establish structures and the energetics of the formation processes. Likewise, calculations were performed on the original $\text{Pd}(\text{en})\text{Br}_2$ system, so as to permit a comparison of the two aqueous solutions from both experimental and theoretical per-

Published online February 20, 2007

Address reprint requests to Dr. Grant N. Merrill, Department of Chemistry, The University of Texas at San Antonio, 6900 North Loop 1604 West, San Antonio, TX 78249, USA. E-mail: grant.merrill@utsa.edu



spectives. This has led to a much more detailed understanding of the hydrolyses of the two palladium(II) complexes. The current results should also contribute to the general knowledge of the structure and reactivity of palladium(II) complexes, where relatively little is known (e.g., stability constants) [22, 23].

Experimental

$\text{Pd}(\text{C}_2\text{N}_2\text{H}_8)\text{Cl}_2$ [15202-99-2] was purchased from Alfa Aesar, Ward Hill, MA (catalog no. 10496) and used without further purification. The stock solution was prepared by dissolving about 1 mmol of $\text{Pd}(\text{en})\text{Cl}_2$ in 10.0 ml of deionized water in a clean, dry glass vial. Deionized water (DI, 18 M Ω) was obtained using a Barnstead Nanopure System (Dubuque, IA). The vial was capped and warmed slightly for 2 d to dissolve the solid. This yielded a 1.0 mM solution of pH 5.2. Experiments were also carried out by dissolving $\text{Pd}(\text{en})\text{Cl}_2$ in D_2O .

The aqueous solutions were investigated using a Finnigan LCQ Duo (Thermo Finnigan, San Jose, CA) quadrupole ion-trap mass spectrometer coupled to an electrospray source. All data were collected and analyzed using the Xcalibur software (San Jose, CA) in full scan and MS/MS modes. The relative collision energy used for CID was uncalibrated and in arbitrary units. Normalized collision energies (NCE) between 10 and 30% were used. The isolation of the parent masses was checked using a NCE of 10% to verify that only the parent ion was present. The following MS conditions were routinely employed: source voltage, 4.5 kV; capillary temperature, 180 °C; capillary voltage, 10.5 V; sheath gas-flow rate, 45 (arbitrary units); and the auxiliary gas-flow rate, 4 (arbitrary units). Solutions were introduced by flow injection at a rate of 5 $\mu\text{L}/\text{min}$. The windows for CID were between 10 and 20 u to isolate all isotopomers for individual complexes. Simulations of the stable isotope patterns were made using the Isotope Viewer in Xcalibur. For the simulated mass spectra, the following default settings were used unless otherwise noted: resolution, ~ 1 Da at 5% height and a + 1 charge.

Computational Methods

All structures were fully optimized at the density functional (B3LYP) [24–26] level of theory. Structures were deemed converged when the root-mean-square (RMS) and maximum component (MAX) of the gradients fell below 0.004 and 0.012 kcalmol $^{-1}\text{\AA}^{-1}$, respectively. To verify that all optimized structures corresponded to minima, Hessians were computed at the same level of theory. Numerical double-differencing of analytical gradients was employed in the calculation of the Hessians. The resulting force constant matrices permitted zero-point energy (ZPE), finite-temperature (FT), and entropic corrections to be computed. The ZPEs and vibrational frequencies were left unscaled. All core electrons were treated with the Stevens, Basch, Krauss, Jasien, and Cundari (SBKJC) effective core potentials (ECP) [27–29]. The valence electrons were modeled with the SBKJC double-split valence basis set to which a single set of d-type polarization functions [30] were added to all atoms except hydrogen and palladium. All calculations were carried out with the GAMESS program [31] running on a Beowulf cluster of personal computers.

Results and Discussion

The mass spectrum obtained by electrospraying an aqueous solution of dichloro(ethylenediamine)palladium(II) ($\text{Pd}(\text{en})\text{Cl}_2$) at pH 5.2 is given in Figure 1, and the significant observed ions are listed in Table 1. (Significance is defined as a percent abundance greater than or equal to 5%.) All the peaks in Table 1 were identified. The base peak (100% abundance) occurs at m/z 436.8 and is consistent with an ion formed from the clustering of $\text{Pd}(\text{en})\text{Cl}_2$ and $\text{Pd}(\text{en})\text{Cl}^+$, i.e., M and $[\text{M} - \text{Cl}]^+$. Further evidence to support this assignment may be found in the peaks at m/z 200.9 and 218.9 with respective abundances of 5 and 80%. The former peak is consistent with $[\text{M} - \text{Cl}]^+$, while the latter is strongly suggestive of an ion formed from the clustering of $[\text{M} - \text{Cl}]^+$ with H_2O .

The peak with the largest m/z ratio (672.8) offers proof for the existence of the trimeric complex $[\text{3M} - \text{Cl}]^+$, formed from two $\text{Pd}(\text{en})\text{Cl}_2$ molecules and one $\text{Pd}(\text{en})\text{Cl}^+$ ion, with an abundance of 15%. It is interesting to note that this trimeric ion is three times more abundant than the monomeric ion, attesting to the strength of the observed ion-molecule interactions.

The peak at m/z 260.9 with a 5% abundance suggests the complexation of the $\text{Pd}(\text{en})\text{Cl}^+$ ion with ethylenediamine, $[\text{M} - \text{Cl} + \text{en}]^+$. A series of peaks corresponding to the apparent sequential loss of HCl from the dimeric $\text{Pd}(\text{en})\text{Cl}_2\text{-Pd}(\text{en})\text{Cl}^+$ ion are seen at m/z 400.9, 364.9, and 328.9. These peak assignments are consistent with the structures $[\text{2M} - \text{Cl} - \text{HCl}]^+$, $[\text{2M} - \text{Cl} - 2\text{HCl}]^+$, and $[\text{2M} - \text{Cl} - 3\text{HCl}]^+$, respectively. It is interesting to note that the percent abundances for these ions do not correlate (inversely) with the number of HCl molecules

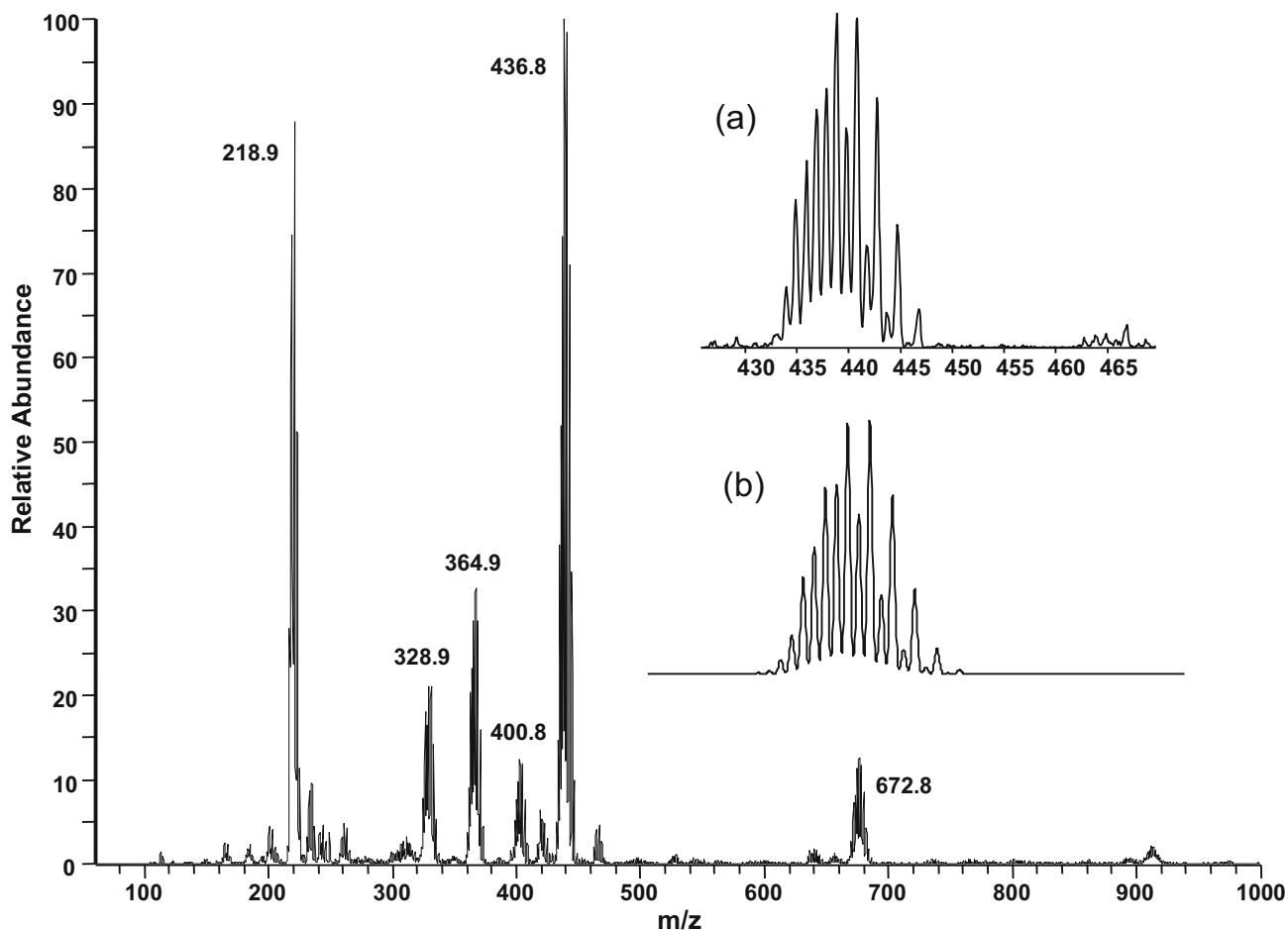


Figure 1. Positive ion mass spectrum of a 1 mM aqueous solution of Pd(en)Cl₂ at pH = 5.2. (a) Expanded region around base peak *m/z* 438.8. (b) Simulated region around base peak.

lost: [2M – Cl – HCl]⁺ = 15%; [2M – Cl – 2HCl]⁺ = 35%; and [2M – Cl – 3HCl]⁺ = 25%. It is unlikely, therefore, that these ions are formed from the loss of HCl from the dimeric [2M – Cl]⁺ ion during the electrospray process

(*vide infra*). A small amount (5%) of the [2M – Cl – HCl]⁺ ion was also found to cluster with H₂O to yield the [2M – Cl – HCl + H₂O]⁺ ion. Density functional theory calculations (*vide infra*) reveal that this reaction is not

Table 1. Observed ions in electrospray mass spectrum (Figure 1) of dilute H₂O solutions of Pd(en)Cl₂ (at pH 5.2). The Pd(en)Br₂ data (at pH 4.4), adapted from Table 1 of Reference [20], is included for purposes of comparison

| Structure | M = Pd(en)Cl ₂ , X = Cl | | | | M = Pd(en)Br ₂ , X = Br | | | |
|---|------------------------------------|-----|--------------|---------|------------------------------------|-----|----------------------------|-----------------|
| | Parent MS | | CID | | Parent MS | | CID | |
| | <i>m/z</i> | % | <i>m/z</i> | % | <i>m/z</i> | % | <i>m/z</i> | % |
| [2M – X] ⁺ | 436.8 | 100 | 400.9, 364.9 | 100, 20 | 568.7 | 100 | 488.7, 408.7, 471.7, 391.7 | 65, 100, 30, 20 |
| [M – X + H ₂ O] ⁺ | 218.9 | 80 | 200.9 | 100 | 262.9 | 70 | 244.9 | 100 |
| [2M – X – 2HX] ⁺ | 364.9 | 35 | 328.9 | 100 | 408.7 | 20 | 328.7 | 100 |
| [2M – X – 3HX] ⁺ | 328.9 | 25 | 296.7 | 100 | | | | |
| [2M – X – HX] ⁺ | 400.9 | 15 | 364.9 | 100 | 488.7 | 15 | 408.7, 471.7, 391.7 | 100, 30, 20 |
| [3M – X] ⁺ | 672.8 | 15 | 436.8 | 100 | 892.2 | 5 | 568.7 | 100 |
| [M – X + en] ⁺ | 260.9 | 5 | | | 305.0 | 45 | | |
| [2M – X – HX + H ₂ O] ⁺ | 420.8 | 5 | | | | | | |
| [M – X] ⁺ | 200.9 | 5 | 162.8 | 100 | 244.9 | 60 | 163.9 | 100 |
| [M – 2X + en] ⁺⁺ | | | | | 113.0 | 25 | | |
| [M – X – HX] ⁺ | | | | | 165.0 | 20 | | |
| [M + en + H] ⁺ | | | | | 384.9 | 15 | | |
| [M – 2X – H + en] ⁺ | | | | | 224.9 | 10 | | |

Table 2. Observed ions in electrospray mass spectra of dilute D₂O solution of Pd(en)Cl₂ at pH 5.2

| Structure | Parent MS | | CID MS | |
|--|------------|-------------|--------------|-------------|
| | <i>m/z</i> | % Abundance | <i>m/z</i> | % Abundance |
| [2M(d8) – Cl] ⁺ | 444.9 | 100 | 407.9, 370.9 | 100, 70 |
| [M(d4) – Cl + D ₂ O] ⁺ | 224.9 | 95 | 204.9 | 100 |
| [M(d4) – Cl] ⁺ | 204.9 | 40 | | |
| [2M(d8) – Cl – 2DCI] ⁺ | 370.9 | 35 | 334.0 | 100 |
| [2M(d8) – Cl – 3DCI] ⁺ | 334.0 | 25 | | |
| [2M(d8) – Cl – DCI] ⁺ | 407.9 | 20 | 370.9 | 100 |
| [M(d4) – Cl – DCI] ⁺ | 167.0 | 20 | | |

particularly exothermic or exoergonic ($\Delta_rH = -15.6$ and $\Delta_rG = -4.8$ kcalmol⁻¹), which offers a ready explanation for why only small amounts of the hydrates are seen for the above ions.

The parent compound was also dissolved in D₂O in an attempt to examine the lability of the amine hydrogen atoms (Figure 2 and Table 2). The base peak was observed at *m/z* 444.9, which was assigned to [2M(d8) – Cl]⁺ dimer. This indicates that all eight of the amine hydrogen atoms were exchanged with deuterium atoms. Other dimeric peaks were observed at *m/z* 407.9, [2M(d7) – Cl – DCI]⁺, *m/z* 370.9, [2M(d6) – Cl – 2DCI]⁺, and *m/z* 334.0, [2M(d5) – Cl – 3DCI]⁺. Monomer peaks were observed at *m/z* 204.9 ([M(d4) – Cl]), and an aqua complex was seen at *m/z* 224.9 [M(d4) – Cl + D₂O]⁺. There is some overlap of the aqua complex with an unidentified complex.

A series of collision-induced dissociation (CID) experiments was undertaken to elucidate the structure and stability of the observed complexes in the full ES mass

spectra. A parent mass isolation width of between 10 and 20 u was used so as to include the full isotope pattern. The isolation of each of the parent mass isotope envelopes was verified using a NCE of 10%. The results from the various MSⁿ experiments are summarized in Table 1 for the experiments done in H₂O and Table 2 for D₂O.

H₂O CID

The trimer, [3M – Cl]⁺, lost M as would be expected for an ES-produced cold cluster. Further CID of the daughter ion, [2M – Cl]⁺, did not produce further loss of M, but losses of HCl instead. There was enough of the trimer available to undertake a series of MSⁿ experiments. The MS³ experiment resulted in a peak observed at *m/z* 400.9 [2M – Cl – HCl]⁺. The next CID step yielded [2M – Cl – 2HCl]⁺ at *m/z* 364.9. MS⁵ yielded *m/z* 328.8 and was the final HCl elimination step. (While MS⁶ experiments also led to daughter ions, their structures

Table 3. Calculated reaction enthalpies (Δ_rH) and free energies (Δ_rG) for experimentally observed ions and related species at 298 K and 1 atm in kcalmol⁻¹

| Ion | Reaction | M=Pd(en)Cl ₂ , X=Cl | | M=Pd(en)Br ₂ , X=Br | |
|---|---|-----------------------------------|--------------------|--------------------------------|--------------------|
| | | Δ_rH | Δ_rG | Δ_rH | Δ_rG |
| [2M – X] ⁺ | M + [M – X] ⁺ → [2M – X] ⁺ | -60.9 | -48.8 | -57.2 | -43.1 |
| [M – X + H ₂ O] ⁺ | [M – X] ⁺ + H ₂ O → [M – X + H ₂ O] ⁺ | -33.9 | -23.5 | -32.7 | -22.2 |
| [2M – X – 2HX] ⁺ | [M – 2HX] + [M – X] ⁺ → [2M – X – 2HX] ⁺ | -69.9 | -57.3 | -54.6 | -42.0 |
| [2M – X – 3HX] ⁺ | [M – HX – X] ⁺ + [M – 2HX] → [2M – X – 3HX] ⁺ | -78.7 | -65.1 | | |
| [2M – X – HX] ⁺ | M + [M – X – HX] ⁺ → [2M – X – HX] ⁺ | -65.2 | -52.9 | -64.3 | -50.8 |
| [3M – X] ⁺ | 2M + [M – X] ⁺ → [3M – X] ⁺ | -47.7 ^a | -41.7 ^a | -45.3 ^a | -38.8 ^a |
| | M + [2M – X] ⁺ → [3M – X] ⁺ | -23.1 ^a | -15.8 ^a | -19.2 ^a | -11.6 ^a |
| [M – X + en] ⁺ | [M – X] ⁺ + en → [M – X + en] ⁺ | -59.5 | -46.1 | -57.7 | -44.1 |
| [2M – X – HX + H ₂ O] ⁺ | [2M – X – HX] ⁺ + H ₂ O → [2M – X – HX + H ₂ O] ⁺ | -15.6 | -4.8 | | |
| [M – X] ⁺ | M → [M – X] ⁺ + X ⁻ | 148.8 | 140.7 | 139.9 | 132.7 |
| [M – 2X + en] ⁺⁺ | [M – 2X] ⁺⁺ + en → [M – 2X + en] ⁺⁺ | | | -137.7 | -123.8 |
| [M – X – HX] ⁺ | [M – X] ⁺ → [M – X – HX] ⁺ + HX | 48.1 | 37.6 | 52.9 | 42.7 |
| [M + en + H] ⁺ | M + en + H ⁺ → [M + en + H] ⁺ | | | -225.1 | -206.0 |
| [M – X – HX + en] ⁺ | [M – X – HX] ⁺ + en → [M – X – HX + en] ⁺ | | | -77.8 | -63.7 |
| | [M – 2X + en] ⁺⁺ → [M – HX – X + en] ⁺ + H ⁺ | | | 109.1 | 100.7 |
| [M – 2HX] | M → [M – 2HX] + 2HX | 101.9 | 67.6 | 111.3 | 67.6 |
| en | M → PdX ₂ + en | 64.8 | 50.9 | 59.5 | 46.8 |
| 2M | M + M → 2M | -36.4 | -22.9 | -31.1 | -15.9 |
| [M – 2X] ²⁺ | M → [M – 2X] ²⁺ + 2X ⁻ | | | 405.7 | 391.3 |

^aB3LYP/SBKJC[d]/HF/SBKJC[d] for [3X-X]⁺.

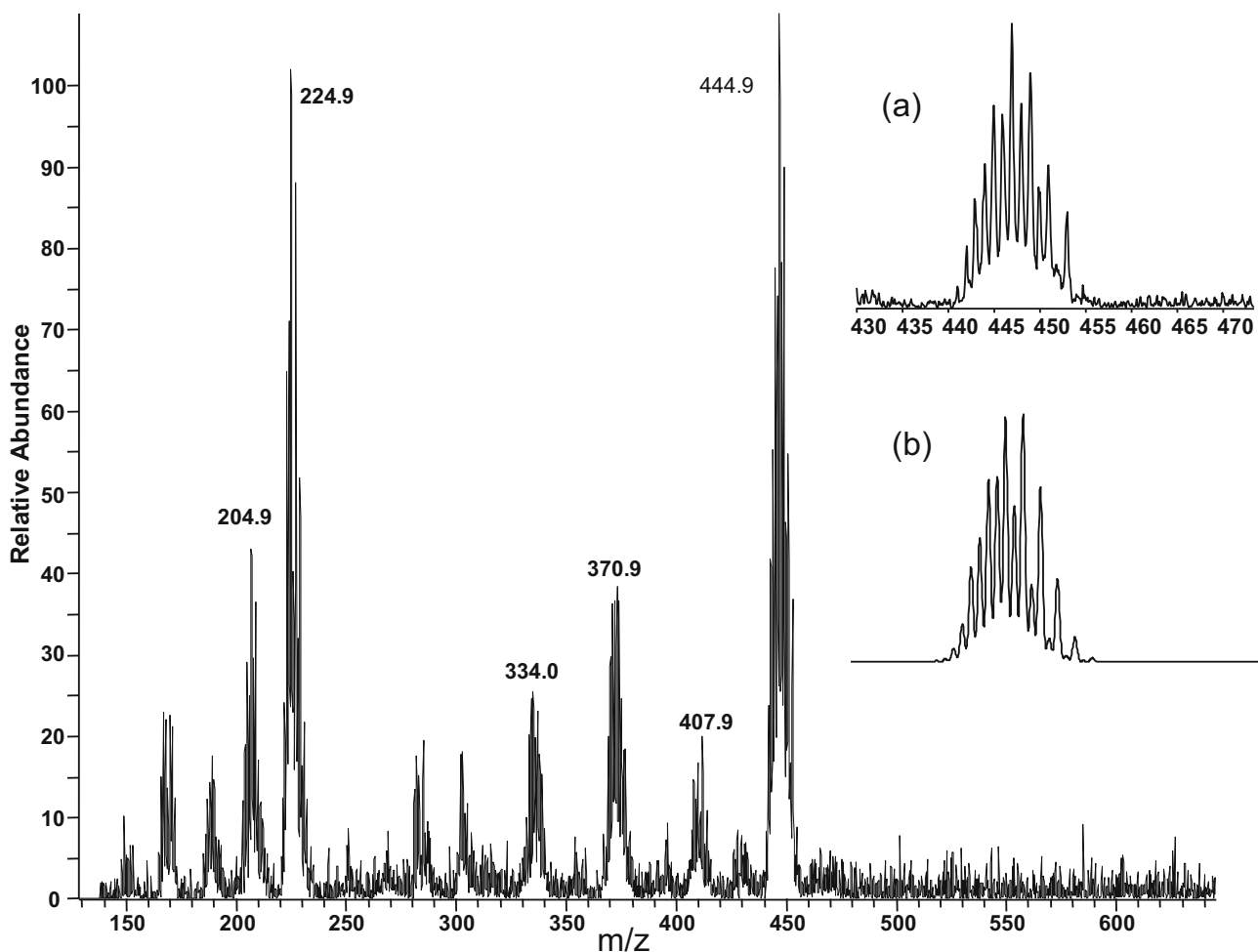


Figure 2. Positive ion mass spectrum of a 1 mM D_2O solution of $Pd(en)Cl_2$ at pH 5.2. (a) Expanded region around base peak of m/z 444.9. (b) Simulated region around base peak.

could not be determined as their low absolute intensities failed to yield complete isotope patterns.)

The CID of $[2M - Cl]^+$ produced by ES yielded $[2M - Cl - HCl]^+$ at m/z 400.9 and $[2M - Cl - 2HCl]^+$ at m/z 364.9. Similar results were observed for $[2M - Cl - HCl]^+$ and $[2M - Cl - 2HCl]^+$ produced by ES; i.e., both lost HCl. Further CID produced similar results to those observed in the trimer CID series. The CID of the $[M - Cl + H_2O]^+$ complex at m/z 218.9 lost 18 m/z units to yield m/z 200.9, $[M - Cl]^+$. The $[M - Cl]^+$ complex was also observed in the full ES spectrum, but there was not enough intensity to carry out additional CID experiments.

A series of low intensity peaks are observed between m/z 200 and 300 in most spectra. These are postulated to belong to a series of complexes containing two ethylenediamine units. At m/z 295.9, $[M + en + H]^+$ is observed. Upon CID the daughter ion observed is $[M + en - HCl]^+$ at m/z 260.9. This ion is also observed in the full ES spectra. When this complex is subjected to CID, a daughter ion is observed at m/z 224.9 and is assigned to $[M - 2HCl + en]^+$. This complex appears in the full ES spectrum, which interferes with the isotopic manifold for $[M - Cl + H_2O]^+$.

D_2O CID

The most notable observation is the up-mass shift of the peaks indicating deuteration of the complexes. The dimer peak shifts to m/z 444.9 indicating the substitution of the eight amine hydrogen atoms of the dimer with eight deuterium atoms. The loss of DCl in the CID experiments also confirms this conclusion. The trimer was not observed. The CID of the $[2M(d8) - Cl]^+$ dimer results in the loss of DCl to yield $[2M(d7) - Cl - DCl]^+$ at m/z 407.9 (100%) and $[2M(d6) - Cl - 2DCl]^+$ at m/z 370.9 (70%). These complexes are also observed in the full ES spectrum. The CID of $[2M(d7) - Cl - 2DCl]^+$ yields $[2M(d6) - Cl - 2DCl]^+$, which in turn led to $[2M(d5) - Cl - 3DCl]^+$ at m/z 334.0 in the MS^3 experiment. The CID of $[M(d4) - Cl + D_2O]^+$ at m/z 224.9 involves the loss of D_2O to produce $[M(d4) - Cl]^+$ at m/z 204.9. The CID of m/z 334 results in weak signals from losses of about twenty m/z units. The isotope patterns in these cases are not well resolved, and therefore we cannot make a determination regarding which neutral was lost.

A rather minimal set of ions and neutrals is required to rationalize the ions observed in the ESMS: M, $[M -$

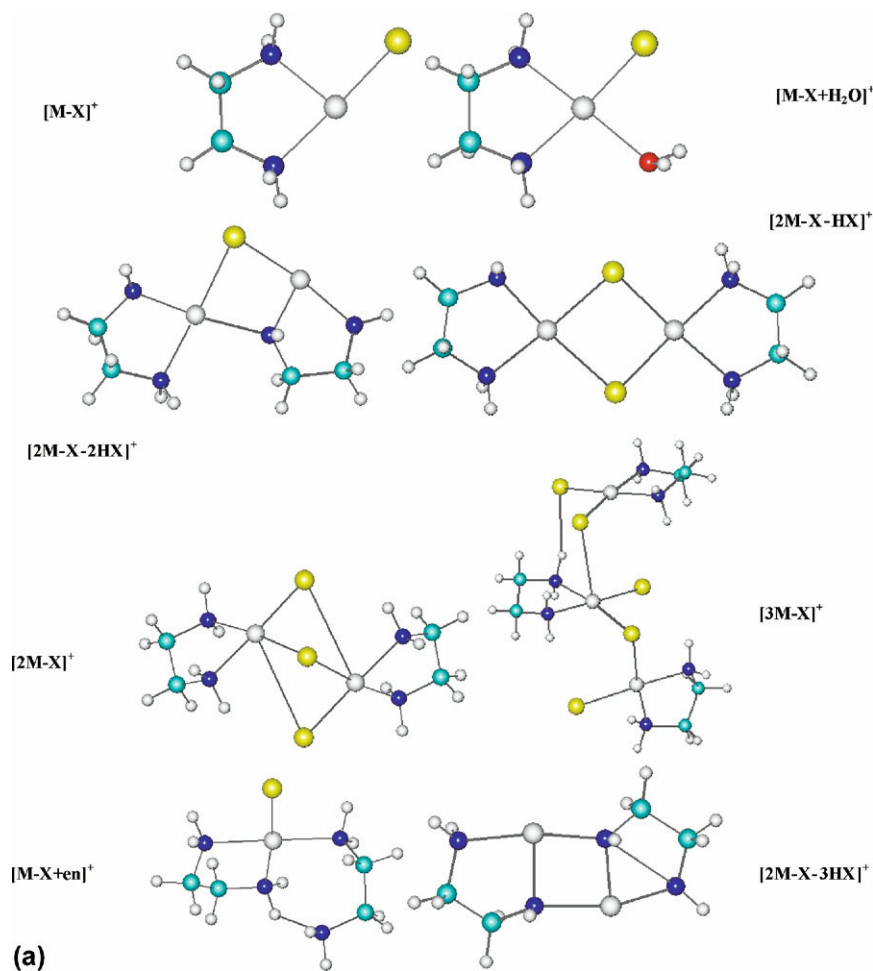
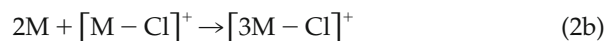
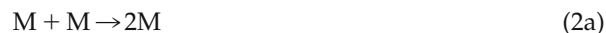
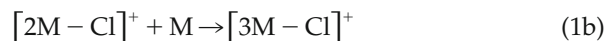
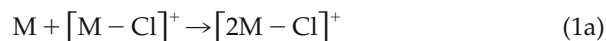


Figure 3. Computed structures for ions seen in experimental mass spectra. Atoms: C = light blue, H = white, N = dark blue, O = red, Br/Cl = yellow, and Pd = grey.

$\text{Cl}]^+$, $[\text{M} - \text{Cl} - \text{HCl}]^+$, $[\text{M} - 2\text{HCl}]^+$, en, and H_2O . We propose therefore that upon acid-catalyzed hydrolysis of $\text{Pd}(\text{en})\text{Cl}_2$ these species are formed; we further hypothesize that, upon dehydration during the electrospray process, clustering of these species leads to the observed mass spectrum (Figure 1).

Table 3 lists the enthalpies and Gibbs free energies of reaction for the formation of the observed ions from the proposed set of species in aqueous solution. These values were computed with density functional theory (DFT). In each reaction, the product ion results from the clustering of a neutral molecule and a cation, and the reactions are therefore exothermic and exoergonic. Figure 3 offers illustrations of the DFT optimized structures of the observed ions, which presumably arise from the reactions given in Table 3. (In lieu of experimental data, the assignment of structures to the observed ions is somewhat tentative. This is especially true for the more complex species, where a greater number of geometric isomers are possible. Systematic searches for these low-energy isomers were conducted, and the proposed structures are thermodynamically feasible.)

While the formation mechanisms for many of the ions ($[2\text{M} - \text{Cl}]^+$, $[\text{M} - \text{Cl} + \text{H}_2\text{O}]^+$, and $[\text{M} - \text{Cl}]^+$) appear rather obvious, a number of the others require comment. The trimeric $[3\text{M} - \text{Cl}]^+$ ion may be formed in a number of manners (eqs 1 and 2)



Given the current experimental data, it is not possible to state definitively which mechanism is operative, but the DFT calculations suggest that both pathways are thermodynamically feasible, i.e., all four reactions are exothermic and exoergonic.

The formation of the $[\text{M} - \text{Cl} + \text{en}]^+$ ion via the reaction in eq 3 is predicated upon the loss of ethylenediamine from $\text{Pd}(\text{en})\text{Cl}_2$ in aqueous solution.

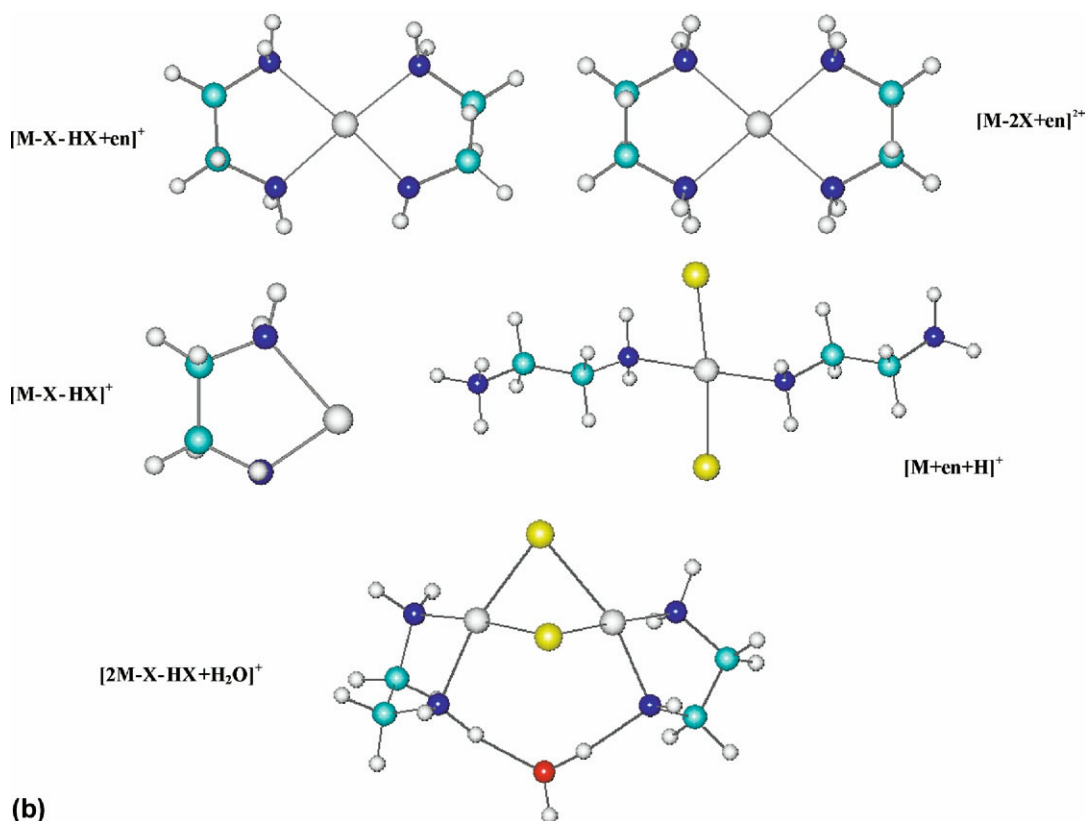
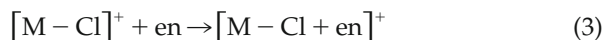


Figure 3. Continued.

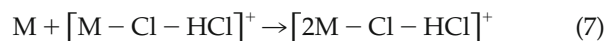
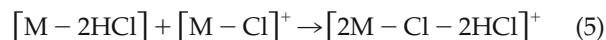


Our calculations predict that the reaction leading to the loss of ethylenediamine from $Pd(en)Cl_2$ (eq 4) is endothermic ($\Delta_r H^0 = 64.8 \text{ kcal mol}^{-1}$) and endoergonic ($\Delta_r G^0 = 50.9 \text{ kcal mol}^{-1}$).



It is, however, 84.0 and 89.8 kcal mol^{-1} less endothermic and endoergonic, respectively, than the loss of Cl^- from M to form the observed $[M - Cl]^+$ ion. (It must be reiterated that these calculations correspond to processes in the gas-phase and solvation effects have not been considered.)

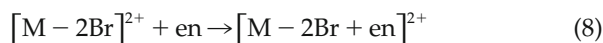
The formation of the series of ions derived from the sequential loss of HCl from the $[2M - Cl]^+$ ion is thermodynamically unfavorable; i.e., the loss mechanisms are all highly endothermic and endoergonic. For example, the loss of HCl from $[2M - Cl]^+$ to form $[2M - Cl - HCl]^+$ is 43.8 and 33.5 kcal mol^{-1} endothermic and endoergonic, respectively. The loss of HCl from the $[2M - Cl]^+$ ion is also inconsistent with the ES experiments, since species with little excess energy are expected to be produced. They can however be rationalized if, in addition to M and $[M - Cl]^+$, $[M - 2HCl]$ and $[M - Cl - HCl]^+$ are present in aqueous solution. The formation of the observed ions can then occur by the reactions in eqs 5, 6, and 7.



The optimized structures in Figure 3 are moreover readily explained if the above three mechanisms are operative.

Using the above paradigm for the formation of the observed ions from the acid-catalyzed hydrolysis of the parent compound, it is possible to offer a more complete picture of the results from our earlier study into the complexes formed by electrospraying dilute aqueous solutions of $Pd(en)Br_2$ (pH 4.4) [20]. A list of the ions observed from the aqueous $Pd(en)Br_2$ solution is given in Table 1, which has been adapted from Table 1 of Reference [20]. If one again assumes that a minimal set of species is formed upon hydration of $Pd(en)Br_2$ under acidic conditions (M, $[M - Br]^+$, $[M - Br - HBr]^+$, $[M - 2HBr]$, en, and H_2O), it is possible to offer reasonable mechanisms for the formation of the observed ions. Additionally, the presence of the $[M - 2Br]^{2+}$ ion and stray protons (pH 4.4) are required. (The $[M - 2Cl]^{2+}$ ion was not seen in the $Pd(en)Cl_2$ spectra nor were protonated products observed.)

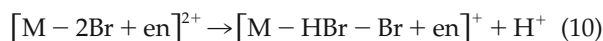
The formation of the observed ions in the Pd(en)Br₂ spectra is postulated to occur by the same general mechanism as hypothesized for the chloro ions: the clustering of a neutral molecule with a cation. The associated enthalpies and (Gibbs) free energies are therefore also predicted to be appreciably exothermic and exoergic, respectively. This is confirmed by the DFT energies (Table 3). With the exception of a few ions not seen in the chloro spectra, all those found in the bromo spectra are formed in similar fashions. The formation of the [M – 2Br + en]²⁺ ion (*m/z* 113.0, 25%) can be accomplished by clustering the [M – 2Br]²⁺ ion with ethylenediamine (eq 8).



This process is calculated to be exothermic ($\Delta_r H^0 = -137.7$ kcalmol⁻¹) and exoergic ($\Delta_r G^0 = -137.7$ kcalmol⁻¹). The existences of the [M + en + H]⁺ (*m/z* 384.9, 15%) and [M – Br – HBr + en]⁺ (*m/z* 224.9, 10%) ions are believed to occur by the attachment and the loss of a proton, respectively, from the [M + en] neutral and [M – 2Br + en]²⁺ ion. The former process (eq 9) corresponds to the (negative) proton affinity (PA) and gas-phase basicity (GB) of the [M + en] neutral and are calculated to be highly exothermic ($\Delta_r H^0 = -225.1$ kcalmol⁻¹) and exoergic ($\Delta_r G^0 = -206.0$ kcalmol⁻¹), respectively.



Similarly, the latter process corresponds to the PA and GB of the [M – 2Br + en]²⁺ ion (eq 10): PA = 109.1 kcalmol⁻¹ and GB = 100.7 kcalmol⁻¹.



Finally, the existence of the [M – Br – HBr]⁺ ion can be accounted for by the loss of HBr from [M – Br]⁺ (eq 11). This reaction is however calculated to be endothermic ($\Delta_r H^0 = 52.9$ kcal/mol) and endoergic ($\Delta_r G^0 = 42.7$ kcal/mol).



For the ions that the chloro and bromo spectra have in common, it is interesting to compare their relative abundances. Both sets of spectra show the dimeric [2M – X]⁺ ion to be in greatest abundance. Once again, the ion in next greatest abundance for both compounds is the [M – X + H₂O]⁺ ion. These commonalities strongly suggest that upon hydration of the Pd(en)X₂ parents, some degree of halide replacement by water is observed. The fact that the bromo spectra exhibit twelve times more of the [M – X]⁺ ion than that seen in the chloro spectra suggest that the hydrolysis is more complete for Pd(en)Br₂. This conclusion is supported by two other observations. First, there appears to be a greater amount of free ethylenediamine in the

Pd(en)Br₂ solutions as witnessed by more than nine times the amount of [M – Br + en]⁺ in the bromo spectra than that observed in the chloro spectra, and the [M – 2X + en]²⁺ ion is only observed in the bromo spectra. Second, the trimeric [3M – X]⁺ ion is three times more prevalent in the chloro spectra. As it is speculated that this ion is formed from the clustering of two M neutrals and one [M – X]⁺ ion (*vide supra*), this again suggest less hydrolysis of the chloro compound. Deeper insights into these differences are currently being sought theoretically; specifically, the hydration enthalpies and (Gibbs) free energies are being computed for palladium(II) complexes, including Pd(en)Cl₂ and Pd(en)Br₂.

The two sets of spectra show the same relative amounts of the [2M – X – HX]⁺ ions (15%) and nearly the same amounts of the [2M – X – 2HX]⁺ ions ([2M – Cl – 2HCl]⁺ = 35% and [2M – Br – 2HBr]⁺ = 20%). Evidence for the presence of the [2M – X – 3HX]⁺ ion (without CID) is only seen in the chloro spectra. These differences may be the result of pH differences in the two aqueous solutions, leading to greater concentrations of the [M – X – HX]⁺ ion in the bromo spectra and the [2M – X – 3HX]⁺ ion in the chloro spectra. This would also help to explain the presence of protonated species in more acidic Pd(en)Br₂ aqueous solutions. The effects of pH on complex formation during the electro-spray process are currently under investigation in our laboratories.

Conclusions

The electrospraying of dilute aqueous solutions of Pd(en)Cl₂ into a quadrupole ion-trap mass spectrometer resulted in the production of a number of Pd(II)-containing ions, the most abundant of which corresponded to the dimeric [2M – Cl]⁺ (100%) and aqua [M – Cl + H₂O]⁺ (80%) ions. These results are similar to those found for an aqueous solution of Pd(en)Br₂.^[20] Additionally, a number of ions corresponding to the apparent sequential loss of HCl were seen in the chloro spectra ([2M – X – nHX]⁺). Once again, a similar series of ions was observed in the bromo spectra. The two sets of spectra did differ in the relative abundances of these ions. Likewise, differences were seen in the percent abundances for the monomeric ions containing more than one en group ([M – Br + en]⁺ and [M – 2Br + en]²⁺), those species involving proton transfer ([M + en + H]⁺ and [M – Br – HBr + en]⁺), and the amount of the trimeric [3M – X]⁺ ion. Pathways for the formation of the observed chloro and bromo ions were offered based upon density functional theory calculations. Both structures and energetics were computed.

Acknowledgments

GNM thanks Dr. Ghezai T. Musie of the Department of Chemistry at the University of Texas at San Antonio for helpful discussions. SBHB expresses his thanks to Mr. Conor P. Mullens of the

Department of Chemistry at the University of Texas at San Antonio for assisting in the mass spectrometry experiments.

References

- Fuertes, M. A.; Alonso, C.; Perez, J. M. Biochemical Modulation of Cisplatin Mechanisms of Action: Enhancement of Antitumor Activity and Circumvention of Drug Resistance. *Chem. Rev.* **2003**, *103*, 645–662.
- Kasparkova, J.; Zehnulova, J.; Farrell, N.; Brabec, V. DNA Interstrand Cross-links of the Novel Antitumor Trinuclear Platinum Complex BBR3464. Conformation, Recognition by High Mobility Group Domain Proteins, and Nucleotide Excision Repair. *J. Biol. Chem.* **2002**, *277*, 48076–48086.
- Rosenberg, B.; Van Camp, L.; Trosko, J. R.; Mansour, V. A. Platinum Compounds: A New Class of Potent Antitumor Agents. *Nature.* **1969**, *222*, 385.
- Milovic, M. N.; Kostic, N. M. Palladium(II) Complexes as a Sequence-Specific Peptidase: Hydrolytic Cleavage Under Mild Conditions of X-Pro Peptide Bonds in X-Pro-Met and X-Pro-Met His Segments. *J. Am. Chem. Soc.* **2003**, *125*, 781–788.
- Zhu, L.; Kostic, N. M. Toward Artificial Metallopeptidases: Mechanisms by which Platinum(II) and Palladium(II) Complexes Promote Selective, Fast Hydrolysis of Unactivated Amide Bonds in Peptides. *Inorg. Chem.* **1992**, *31*, 3944–4001.
- Pettit, L. D.; Bezer, M. Complex Formation Between Palladium(II) and Amino Acids, Peptides, and Related Ligands. *Coord. Chem. Rev.* **1985**, *61*, 97–114.
- Appleton, T. G.; Bailey, A. J.; Bedgood, J.; Danny, R.; Hall, J. R. Amino Acid Complexes of Palladium(II). 1. NMR Study of Reactions of the Diaqua(Ethylenediamine) Palladium(II) Cation with Ammonia, Betaine, and the Amino Acids $^+H_3N(CH_2)_nCO_2^-$ ($n = 1-3$). *Inorg. Chem.* **1994**, *33*, 217–226.
- Wyatt, K. S.; Harrison, K. N.; Jensen, C. M. Release of Platinum from Cysteine Residues Induced by N,S-Donor Chelation. *Inorg. Chem.* **1992**, *31*, 3867–3868.
- Martin, R. B. Platinum Complexes: Hydrolysis and Binding to N(7) and N(1) of Purines; Wiley VCH: New York, 1999, pp 183–205.
- Djuran, M. I.; Lempers, E. L. M.; Reedijk, J. Reactivity of Chloro- and Aqua(Diethylenetriamine) Platinum(II) Ions with Glutathione, S-Methylglutathione, and Guanosine 5'-Monophosphate in Relation to the Antitumor Activity and Toxicity of Platinum Complexes. *Inorg. Chem.* **1991**, *30*, 2648–2652.
- Rochon, F. D.; Buculei, V. Multinuclear Magnetic Resonance Spectroscopy and Crystal Structures of Iodo-Bridged Dinuclear Pt(II) Complexes with Amines. *Inorg. Chim. Acta.* **2005**, *358*, 3919–3926.
- Over, D.; Bertho, D. G. Fixing the Conformations of Diamineplatinum(II)-GpG Chelates: NMR and CD Signatures of Individual Rotamers. *J. Biol. Inorg. Chem.* **2006**, *11*, 139–152.
- Tsierkezos, N. G.; Schröder, D.; Schwarz, H. Complexation of Nickel(II) by Ethylenediamine Investigated by Means of Electrospray Ionization Mass Spectrometry. *Int. J. Mass Spectrom.* **2004**, *235*, 33–42.
- Tercero-Moreno, J. M.; Matilla-Hernández, A.; González-García, S.; Nicolás-Gutiérrez, J. Hydrolytic Species of the Ion Cis-Diaqua(Ethylenediamine) Palladium(II) Complex and of Cis-Dichloro(Ethylenediamine) Palladium(II): Fitting Its Equilibrium Models in Aqueous Media with or without Chloride Ion. *Inorg. Chim. Acta.* **1996**, *253*, 23–29.
- Giacomelli, A.; Malatesta, F.; Spinetti, M. C. Solution Reactions at Palladium(II) Complexes Producing Dimeric Species: Stability Constants Determination for Simultaneous Equilibria. *Inorg. Chim. Acta.* **1981**, *51*, 55–60.
- Anderegg, G. The Stability of the Palladium(II) Complexes with Ethylenediamine, Diethylenetriamine, and Tris(β -Aminoethyl)-Amine. *Inorg. Chim. Acta.* **1986**, *111*, 25–30.
- Tercero, J. M.; Matilla, A.; Sanjuán, M. A.; Moreno, C. F.; Martín, J. D.; Walmsley, J. A. Synthesis, Characterization, Solution Equilibria, and DNA Binding of Some Mixed-Ligand Palladium(II) Complexes. Thermodynamic Models for Carboplatin Drug and Analogues Compounds. *Inorg. Chim. Acta.* **2003**, *342*, 77–87.
- Henderson, W.; Sabat, M. Platinum(II)- and Palladium(II)-Amide Complexes $[M\{NC(O)CH_2CH_2CH_2\}_2L_2]$ Derived from 2-Azetidinone (β -Propiolactam); a Synthetic, Electrospray Mass Spectrometric and X-Ray Crystallographic Study. *Polyhedron* **1997**, *16*, 1663–1677.
- Vrkic, A. K.; O'Hair, R. A. J. Gas Phase Ion Chemistry of Para Substituted Benzene Diazonium Ions, Their Salt Clusters, and Their Related Phenyl Cations. *Int. J. Mass Spectrom.* **2002**, *218*, 131–160.
- Bach, S. B. H.; Sepeda, T. G.; Merrill, G. N.; Walmsley, J. Complexes of Dibromo (Ethylenediamine) Palladium (II) Observed from Aqueous Solutions by Electrospray Mass Spectrometry. *J. Am. Soc. Mass Spectrom.* **2005**, *16*, 1461–1469.
- Henderson, W.; Nicholson, B. K.; McCaffrey, L. J. Applications of Electrospray Mass Spectrometry in Organometallic Chemistry. *Polyhedron* **1998**, *17*, 4291–4313.
- Stypinski-Mis, B.; Anderegg, G. The Stability of Palladium(II) Complexes with Sulfur-Containing Ligands. *Anal. Chim. Acta.* **2000**, *406*, 325–332.
- Pankratov, A. N.; Borodulin, V. B.; Chaplygina, O. A. A Quantum Chemical Consideration of Ligand Exchange in Palladium(II) Aqueous and Chloride Complexes. *J. Coord. Chem.* **2004**, *57*, 833–842.
- Becke, A. D. Density-Functional Exchange-Energy Approximation with Correct Asymptotic Behavior. *Phys. Rev.* **1988**, *A38*, 3098–3100.
- Lee, C.; Yang, W.; Parr, R. G. Development of the ColleSalvetti Correlation-Energy Formula into a Functional of the Electron Density. *Phys. Rev.* **1988**, *B37*, 785–789.
- Becke, A. D. A New Mixing of Hartree-Fock and Local-Density-Functional Theories. *J. Chem. Phys.* **1993**, *98*, 1372–1377.
- Stevens, W. J.; Basch, H.; Krauss, M. J. Compact Effective Potentials and Efficient Shared-Exponent Basis Sets for the First- and Second-Row Atoms. *J. Chem. Phys.* **1984**, *81*, 6026–6033.
- Stevens, W. J.; Krauss, M. J.; Basch, H.; Jasien, P. G. Relativistic Compact Effective Potentials and Efficient, Shared-Exponent Basis Sets for the Third-, Fourth-, and Fifth-Row Atoms. *Can. J. Chem.* **1992**, *70*, 612–630.
- Cundari, T. R.; Stevens, W. J. Effective Core Potential Methods for the Lanthanides. *J. Chem. Phys.* **1993**, *98*, 5555–5565.
- Hariharan, P. C.; Pople, J. A. The Influence of Polarization Functions on Molecular Orbital Hydrogenation Energies. *Theor. Chim. Acta.* **1973**, *28*, 213–222.
- Schmidt, M. W.; Baldridge, K. K.; Boatz, J. A.; Elbert, S. T.; Gordon, M. S.; Jensen, J. H.; Koseki, S.; Matsunaga, N.; Nguyen, K. A.; Su, S.; Windus, T. L.; Montgomery, J.; Dupuis, M. General Atomic and Molecular Electronic Structure System. *J. Comput. Chem.* **1993**, *14*, 1347–1363.